



K-law spectral signature correlation algorithm to identify white spot syndrome virus in shrimp tissues

Mario A. Bueno-Ibarra ^a, M. Cristina Chávez-Sánchez ^{b,*}, Josué Álvarez-Borrego ^c

^a Centro Interdisciplinario de Investigación para el Desarrollo Integral Regional (CIIDIR-Sinaloa), Departamento de Biotecnología Agrícola, Bioinformática, Blvd. Juan de Dios Bátiz Paredes #250, Col. San Juachín, Guasave Sinaloa, C.P. 81101, Mexico

^b Centro de Investigación en Alimentación y Desarrollo A. C. (CIAD), Unidad Mazatlán en Acuicultura y Manejo Ambiental, Sábalo Cerritos S/N, Apdo. Postal 711, Estero del Yugo, Mazatlán Sinaloa, C.P. 82010, Mexico

^c Centro de Investigación Científica y de Educación Superior de Ensenada (CICESE), División de Física Aplicada, Departamento de Óptica, Carretera Ensenada-Tijuana No. 3918, Fraccionamiento Zona Playitas, Ensenada, Baja California, C.P. 22860, Mexico

ARTICLE INFO

Article history:

Received 21 March 2011

Received in revised form 7 May 2011

Accepted 10 May 2011

Available online 18 May 2011

Keywords:

White spot syndrome virus

Inclusion bodies

Digitalized images

Spectral signature

ABSTRACT

An algorithm is developed to identify the white spot syndrome virus (WSSV) inclusion bodies, found in shrimp tissues by the analysis of digitalized images from infected samples. WSSV slide images were acquired by a computational image capture system and a new identification algorithm is developed to obtain those infected shrimp samples by the quantitative measurement of the complexity pattern found in WSSV inclusion bodies. Representative groups of WSSV inclusion bodies from infected shrimp tissues and organs were analyzed.

© 2011 Elsevier B.V. All rights reserved.

1. Introduction

Since 1992 to date, have been reported near to twenty viruses to infect marine shrimps, however just seven of these viral pathogens are currently mentioned by the World Organization for Animal Health (OIE) as causing important losses in the shrimps population (OIE, 2010). White spot syndrome (WSSV) is by far the most devastating pathogen of the farmed shrimp, affecting the economy of shrimp producers around the world restraining aquaculture production (Walker and Mohan, 2009). White spot syndrome disease is an infection caused by the virus named WSSV, which is the only member of the *Nimaviridae* family. The virions have a double strain of DNA, are ovoid, ellipsoid or bacilliform in shape, have a trilaminar membrane and measure 120–150 × 270–290 nm in size. The genome size is approximately 290 kbp. The epidemics is characterized by a rapid and increase mortality showing symptoms of anorexia, lethargy, in some cases Asian species shows the presence of white spots in the cephalothorax as characteristic of the disease, while in the American species of penaeids, infected or moribund shrimp have reddish coloration due to the expansion of chromatophore (Lightner, 1996; Lightner and Pantoja, 2001; OIE, 2010). WSSV can spread and infect shrimps of any stage of grow-out, asymptotically affecting all life cycle stages, from eggs to

broodstock. Once the clinical signs are developed, mortality can reach 100% in 3 days. WSSV is a highly contagious viral disease of penaeid prawns (Penaeidae family), However, all decapod crustaceans including prawns, lobsters and crabs from marine, brackish water or fresh water are considered susceptible to the infection (OIE, 2010).

In México, several shrimp producers from Sonora, Sinaloa and Nayarit states reflected their losses by the reduction of exportations from 30 million USD in 2000 compared to the 45 million USD in 1999, the losses amount were approximately 15 million USD just in one production year. After this year producers, authorities and academy have been taking actions to control the WSSV disease to reduce the impact, however still is causing important losses. Sinaloa has lost by the impact of this virus the amount of \$5,059,956,000 from 2003 to 2009 (Aquatic Health Committee of Sinaloa State (CESASIN), 2010, personal communication). The state of Sonora has lost by the same pathogen a total of \$1,800,000,000 in 2004 to 2010 (Aquatic Health Committee of Sonora State (COAES), 2010, personal communication). Baja California Sur State lost during one outbreak of WSSV in 2008, the amount of 30 tons so entailed a loss of about \$1,500,000 (Aquatic Health Committee of Baja California Sur (CESABCS), 2010, personal communication). Information is not available from Nayarit State, but there is no doubt that the effects had also similar impact.

Several techniques have been implemented and developed for viral and bacterial penaeid shrimps diagnostics; these can be divided in traditional morphological pathology, bioassay, microbiology, molecular methods such as polymerase chain reaction (PCR) and implementation

* Corresponding author.

E-mail addresses: mbueno@ipn.mx (M.A. Bueno-Ibarra), marcris@ciad.mx (M.C. Chávez-Sánchez), josue@cicese.mx (J. Álvarez-Borrego).

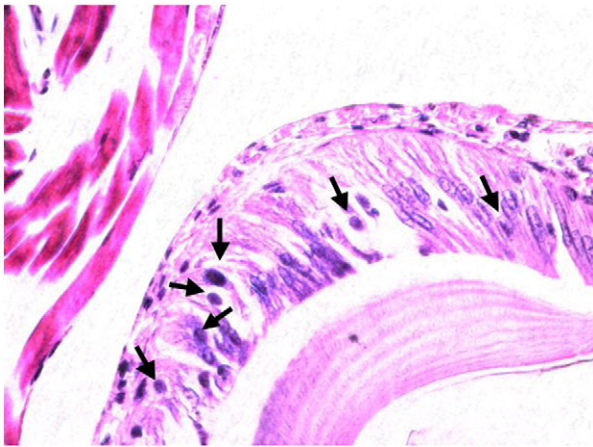


Fig. 1. Arrows show the effects of WSSV infection on cuticular epithelium cells from a histological shrimp tissue sample.

of monoclonal antibodies (Mabs) for the detection of WSSV in slices of paraffin (Lightner, 1996; OIE, 2010), however three methods are used traditionally for WSSV diagnostics: histological analysis, in situ hybridization on fixed tissues with WSSV specific gene probes and PCR method with specific oligonucleotide primers (Poulos et al., 2001).

Histology is still considered the common tool in medical and veterinary for research and diagnostics tasks (Lightner and Redman, 1998). Sometimes for massive diagnostic requirements or epidemiological studies requires a considerable amount of slides that have to be analyzed to determine pathological changes in several tissue cells or to allow the pathogen identification which are sometimes difficult to recognize with other alternative techniques. For this kind of analysis the method involves several steps to obtain the final sample, which is a tissue slice of 5 μm thickness, stained with hematoxylin–eosin necessarily to make the examination under microscope (Bell and Lightner, 1988; Lightner, 1996; Lightner and Redman, 1998), as shown in Fig. 1.

WSSV infection is commonly seen in cuticular epithelial cells and connective tissue cells of the stomach and gills. However it is also seen in antennal gland, lymphoid organ, hematopoietic tissue and phagocytes of the heart. Infected cells typically have hypertrophied (enlarged) nuclei containing a single intranuclear inclusion. Inclusions at the beginning are eosinophilic and sometimes are separated by a clear halo beneath the nuclear membrane; these are known as Cowdry type A inclusions. Later inclusions become lightly to deeply basophilic and fill the entire nucleus (Lightner and Pantoja, 2001; OIE, 2010), as shown in Fig. 2.

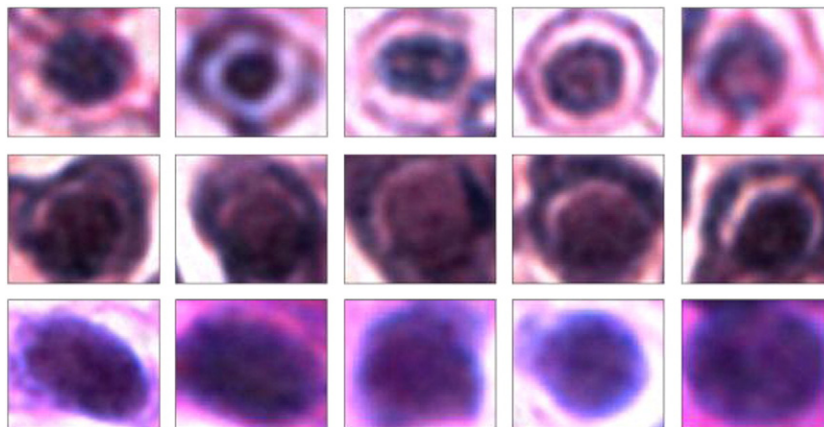


Fig. 2. WSSV basophilic and Cowdry type A inclusion bodies.

The need for rapid, sensitive diagnostic methods led to develop new alternative techniques in different fields of knowledge like computing optic disciplines, which can be of support to conventional methods. Several optic and computational techniques were developed to recognize these kinds of biological patterns, the analysis of inclusion bodies is determinant of the virus presence, thus color correlation approach was used to analyze and recognize the presence of Infectious Hypodermal and Hematopoietic Necrosis Virus (IHHNV) inclusion bodies by histological samples from 35 mm transparencies digitalized with a flatbed scanner (Álvarez-Borrego and Chávez-Sánchez, 2001) as well as WSSV color images are obtained and analyzed in this paper.

The aim of this manuscript is to show a new computer algorithm capable to analyze several shrimp tissue samples infected by WSSV basophilic and Cowdry type A inclusion bodies acquired from histological digitalized color images, by applying Fourier spectral filtering techniques over these slide samples, such as K-Law nonlinear filter.

These Fourier spectral and color correlation techniques have demonstrated the capability to analyze important characteristics from viruses and pathogens (Álvarez-Borrego and Chávez-Sánchez, 2001; Mouriño-Pérez et al., 2006), including applications in several fields (Coronel-Beltrán and Álvarez-Borrego, 2010; Millán et al., 1992).

2. Materials and methods

2.1. Virus sample preparation

Experimental shrimps were obtained from a farm located in the state of Sinaloa, México; transported alive to the laboratory to be fixed in Davidson's solution; after 24 h, the fixative was discarded and shrimps were preserved in 50% alcohol solution until they were ready to be processed by conventional histology techniques, as suggested by Lightner (1996) and Lightner and Redman (1998).

Once histological slides were prepared and ready to be examined under microscope, different types of WSSV inclusion bodies were selected from cuticular epithelium, connective tissue and abdomen tissue, afterwards multispectral digitalized images were obtained to construct a comparison inclusion bodies filter bank; subsequently several images were acquired from the shrimp's slide samples to be diagnosed by KSCA, like WSSV shrimp's infected tissue image, as shown in Fig. 1.

2.2. Digitalized images capture

The WSSV slide images were acquired by a computational system of capture images as shown in Fig. 3, including proprietary image processing software, to enhance the digitalized images with novel



Fig. 3. Leica microscope model DMRXA2 equipped with a RGB color 3.2 mega pixel digital camera (Leica model DC 300) attached to a 2.5 GHz PC Pentium IV.

autofocus and fusion of the developed techniques by Bueno-Ibarra et al. (2005a,b) running inside a 2.5 GHz PC Pentium IV with 1 GByte RAM and 80 GBytes HD, attached to a fully automated research Leica microscope (model DMRXA2) equipped with a 3.2 mega pixel RGB color digital camera (Leica model DC 300). The microscope also performs multi-parameter measurements combining specimen selection, scanning, and focusing, for entirely automatic operations these characteristics make a full degree of automation permitting to create a new kind of algorithms like those developed by Bueno-Ibarra et al. (2005a,b).

A set of 110 microscope field images of single inclusion bodies were acquired from the slides of infected shrimp's tissues by 60× objective with a 2088 × 1550 pixels resolution Leica DC 300 digital color camera, e.g., as shown in Fig. 1; each representative image elected to build the WSSV inclusion body filter bank can contain about an average from 30 to 60 approximately WSSV inclusion bodies depending of the level of infection. Afterwards, a set of 870 WSSV inclusion body images were selected from the inside of these 110 previous acquired slide images to build a filter bank containing a set of 100 most representative WSSV inclusion body images, like those shown in Fig. 2.

2.3. K-Law spectral correlation algorithm to WSSV identification

KSCA is divided by two main process: in an initial process some candidate spatial regions of WSSV infected shrimp's image (ISI) that were analyzed are identified in rough manner; each candidate spatial region can be a potential WSSV inclusion body identified by KSCA, afterwards these candidate spatial regions are registered and marked as target to be analyzed under the KSCA's second process for a better and finest identification; this deep analysis is done by calculating the WSSV K-Law Spectral Signature Index i^{SS} (Bueno-Ibarra et al., 2010), however part of mathematical basis is explained in this paper.

2.3.1. K-Law spectral correlation initial process

Let us introduce some useful definitions and functions required in the initial process: intensity spatial domain matrix data of each WSSV ISI were obtained to be analyzed by KSCA; thus multispectral function $F^\lambda(x,y)$ is defined for every pixel coordinates x and y on digitalized ISI (problem images, e.g., as shown in Fig. 1), where $\lambda = \{\lambda_R, \lambda_G, \lambda_B\}$ acquired by a CCD's digital camera with range [0, 255] and red (R), green (G) and blue (B) are channels in RGB color space representation.

Let $F_1^\lambda, F_2^\lambda, F_3^\lambda, \dots, F_w^\lambda$ be the multispectral functions set of W captured ISIs of size $M \times N$ pixels; $F_i^\lambda(x,y)$ is the captured image matrix with pixels (x,y) in the i^{th} order, inside W set, where $x = 1, \dots, M, y = 1, \dots, N$ and $i = 1, \dots, W$.

Let $F_i^\lambda(x,y)$ be decomposed in their respectively RGB channels $\{\lambda_R, \lambda_G, \lambda_B\}$, obtaining the intensity matrix data $\{I^{R_i}(x,y), I^{G_i}(x,y), I^{B_i}(x,y)\}_i$ of each ISI, where the spectral properties are analyzed. Afterwards, $I_i^{G_i}(x,y)$ green channel intensity matrix is obtained, where WSSV inclusion bodies

are well characterized, reflecting a set of clear spectral signatures (Bueno-Ibarra et al., 2010).

Let $I_i^{G_i}(x,y)$ function be defined such as enhancement intensity matrix function after $I_{Mask}^{G_i}(x,y)_i$ is applied over $I_i^{G_i}(x,y)$ by a threshold value τ , thus $I_{Mask}^{G_i}(x,y)_i \in [0, 1]$ can be expressed as

$$I_{Mask}^{G_i}(x,y)_i = \{I_i^{G_i}(x,y) < \tau | \tau \in \mathbb{Z}^+ \wedge 0 \leq \tau \leq 255\}. \quad (1)$$

Changing the threshold value τ makes possible to enhance the inclusion body attributes and to get better results in WSSV identification. Thereby, $I_i^{G_i}(x,y)$ can be obtained as follow

$$I_i^{G_i}(x,y) = I_i^{G_i}(x,y) \Delta I_{Mask}^{G_i}(x,y)_i, \quad (2)$$

where Δ represents the bitwise multiplication.

Until this point of the process, the ISIs obtained have been manipulated to 3.2 megapixels, the KSCA has the capacity to process high resolution images, but in real time processing the KSCA takes much more time when processing a whole high resolution image, thus the KSCA optimization procedure segments the high resolution ISI in several sub images to build a tiled matrix of images.

Let $\{T_{j,i}^{G_i}(x,y) | j = 0, 1, \dots, J \wedge l = 0, 1, \dots, L\}$ be the set of sub images or tiles that integrates the $I_i^{G_i}(x,y)$ intensity matrix function; $J \times L$ image tiles are included in tiled matrix, thus each separated tile is processed, speeding the process time of the KSCA.

K-Law nonlinear filter function (K-Law) in pattern recognition is used to analyze particularly discriminating characteristics of patterns under analysis (González-Fraga et al., 2006; Solorza and Álvarez-Borrego, 2010), like each filter created from WSSV inclusion bodies.

K-Law filter function is derived by the Fourier transform, thus the K-Law nonlinear filter of $T_{j,i}^{G_i}(x,y)$ is denoted by

$$T_{j,i}^{G_i}(u,v) = |T_{j,i}^{G_i}(u,v)|^k \exp[-i\phi(u,v)], \quad k = 0.1, \quad (3)$$

where k is the nonlinear strength, not included in the classical Fourier transform, thus changing the k value, $0 < k < 1$ in Eq. (3), permits the variability of filter features; intermediate values of k increase the discriminate capacities of the KSCA [22,23].

Let $t_{j,i}^{G_i}(u,v)$ function be defined by the application of K-Law Fourier related filter, calculated over the $T_{j,i}^{G_i}(x,y)$ denoted by

$$t_{j,i}^{G_i}(u,v) = T_{j,i}^{G_i}(u,v), \quad 0 < k < 1 \quad (4)$$

where $k = 0.1$ is used in Eq. (4) and u, v are variables in frequency domain.

Let $g_1^{G_i}, g_2^{G_i}, g_3^{G_i}, \dots, g_p^{G_i}$ be defined such as set of WSSV inclusion bodies filter bank that will be analyzed by KSCA, like those shown in Fig. 2. Thus, P is the number of WSSV inclusion bodies contained inside

the filter bank and the function $g_q^{\lambda^c}(x',y')$ with pixels (x',y') be the WSSV inclusion body image filter located in the q^{th} position inside filter bank.

Cross correlation of two multispectral signals in complex plane; U^{λ^β} and O^{λ^β} is given in each channel as

$$CC^{\lambda^\beta}(x,y) = \mathfrak{F}^{-1} \left(U^{\lambda^\beta}(u,v) \cdot O^{*\lambda^\beta}(u',v') \right), \tag{5}$$

where $\beta = R, G, B$ are respectively red, green and blue channels, (u,v) and (u',v') are coordinates in the Fourier plane, point to point multiplication is given by $\{\bullet\}$, symbol $\{*\}$ is the complex conjugate of function O^{λ^β} and operator \mathfrak{F}^{-1} is the inverse Fourier transform; thus, if the $CC^{\lambda^\beta}(x,y)$ correlation is positive we are going to find maximum correlation peak in the same position of object coordinates, as shown in Fig. 4.

WSSV inclusion body identification is given by the application of Eq. (5), correlating every $g_q^{\lambda^c}(x',y')$ WSSV filter function against every tile image $T_{j,i}^{\lambda^c}(x,y)$ function in complex plane.

Let $KSC^{\lambda^c}(x,y)$ function be defined as K-Law Spectral Correlation (KSC), denoted by

$$KSC^{\lambda^c}(x,y) = \mathfrak{F}^{-1} \left(t_{j,i}^{\lambda^c}(u,v) \cdot g_q^{*\lambda^c}(u',v') \right), \tag{6}$$

where $t_{j,i}^{\lambda^c}(u,v)$ is calculated using Eq. (4) and $g_q^{*\lambda^c}(u',v')$ is the complex conjugate of $\mathfrak{F}^k \{ g_q^{\lambda^c}(x',y') \}$ with $k=0.1$; \mathfrak{F}^k is the K-Law Fourier transform of WSSV inclusion body filter.

Finally, let KSC^v be defined as the magnitude value of $KSC^{\lambda^c}(x,y)$ used to measure the WSSV inclusion body identification strength used by the initial process of KSCA, it can be denoted as

$$KSC^v = \left| \max \left(KSC^{\lambda^c}(x,y) \right) \right|, \tag{7}$$

where $\max\{\}$ function get the maximum peak from $KSC^{\lambda^c}(x,y)$ matrix located in (x,y) coordinates; if the correlation peak has a low value it can increase the sensibility doing $|KSC^v|^2$. Thus if the maximum peak from $|KSC^v|^2 > \zeta$, where ζ is a threshold cross correlation value, it means that we have a positive WSSV inclusion body identification.

2.3.2. K-Law spectral correlation second process

Let $\{S(x^c,y^c)_1, S(x^c,y^c)_2, \dots, S(x^c,y^c)_\Psi\}$ be defined as WSSV inclusion bodies identified vector by KSCA initial process, where $S(x^c,y^c)_s$ is WSSV inclusion body identified (WIBI) image area centered in (x^c,y^c) coordinates, where Ψ is a vector length of WIBIs and $s = 1, \dots, \Psi$.

Spectral signature index i^{ss} is defined by

$$i^{ss} = \left\{ \frac{SSF(f^{\lambda^c}(u,v))}{(A_{Mask})} \mid (u,v) \in \mathbb{C} \right\}, \tag{8}$$

where SSF function is defined by

$$SSF(f^{\lambda^c}(u,v)) = \begin{cases} 1, & \text{if } \text{Re}(f^{\lambda^c}(u,v)) > 0 \\ 0, & \text{otherwise} \end{cases}, \tag{9}$$

and A_{Mask} is defined by

$$A_{Mask} = \sum_{x,y} I_{Mask}^{\lambda^c}(x,y), \text{ for } I_{Mask}^{\lambda^c}(x,y) > 0, \tag{10}$$

and $f^{\lambda^c}(x,y)$ is the WSSV inclusion body image contained in WSSV filter bank.

The significance of this spectral index of Eq. (8) is owing to the calculation of the proportional WSSV texture frequencies of Eq. (9), divided by the virus inclusion body area calculated in Eq. (10), thus the index gives us a tissue damage signature not found in a healthy shrimp's tissue. After several statistical analysis and measurements, the i^{ss} is established in well defined fringe $1.3853 \leq i^{ss} \leq 2.1143$ with $(\pm 2SE)$ (Bueno-Ibarra et al., 2010), where the standard error is defined by $SE = \sigma / \sqrt{n}$ of the infected sample tissues analyzed by the Cowdry type A inclusion bodies, like as shown in Fig. 2.

Let $i^{ss}(S(x^c,y^c)_s)$ function be defined as the value obtained by the analysis on every WIBI, then can be stated by

$$D = \begin{cases} 1, & \text{if } 1.3853 \leq i^{ss}(S(x^c,y^c)_s) \leq 2.1143 \\ 0, & \text{otherwise} \end{cases}, \tag{11}$$

where D is the diagnosis result, thus if $D = 1$ a positive WSSV inclusion body is found.

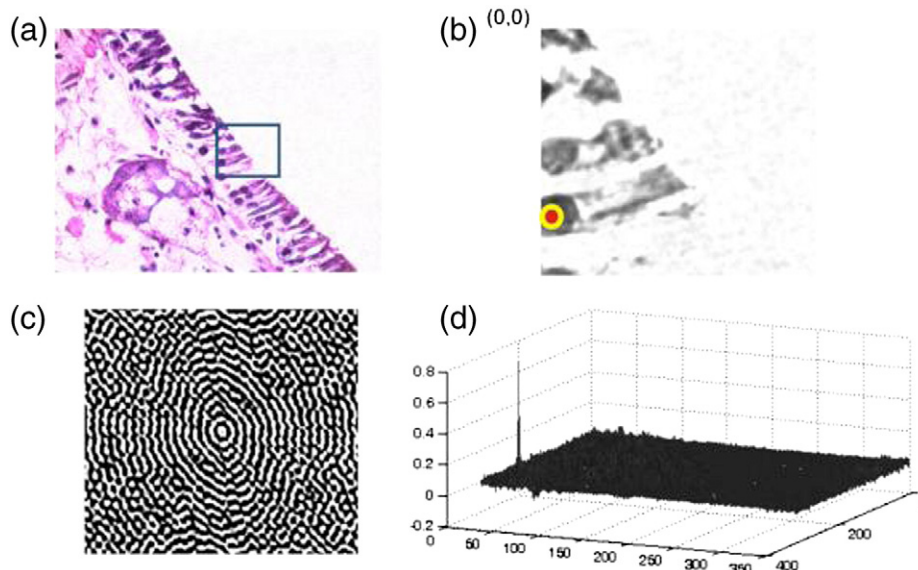


Fig. 4. K-Law Spectral Correlation function calculated in tile image; (a) Shrimp's tissue microscopic image under analysis by KSCA, (b) Tiled image extracted from (a), to be analyzed, indicating the KSC peak with a blue circle, (c) K-Law WSSV inclusion body filter in complex plane under identification, and (d) KSC peak obtained by KSC function.

2.3.3. K-Law spectral correlation diagram

Fig. 5 shows the process block diagram of the algorithm proposed involved in WSSV inclusion bodies identification by the Fourier K-Law non linear filtering correlation. This methodology is explained by the following steps: 1) $F_1^\lambda, F_2^\lambda, F_3^\lambda, \dots, F_w^\lambda$ shrimp's tissues set to be analyzed are acquired by Leica DC 300 color camera; 2) every $F_i^\lambda(x, y)$ function analyzed at once is divided into their respectively RGB $I_i^{\lambda r}(x, y), I_i^{\lambda g}(x, y)$ and $I_i^{\lambda b}(x, y)$ channels; 3) using $I_{Mask}^{\lambda g}(x, y)$ mask image function enhancement operation over $I_i^{\lambda g}(x, y)$ green channel intensity function is obtained the $Ie_i^{\lambda g}(x, y)$ intensity function; 4) tiled matrix operation is applied over $Ie_i^{\lambda g}(x, y)$ intensity function by KSCA to analyze high resolution WSSV images; 5) each tile $T_{j,l}^{\lambda g}(x, y)$ is extracted to be analyzed one by one; 6) corresponding K-Law nonlinear operation is applied over $T_{j,l}^{\lambda g}(x, y)$ by $\mathfrak{F}^k\{T_{j,l}^{\lambda g}(x, y)\}$ to get $t_{j,l}^{\lambda g}(u, v)$ tile intensity function in complex plane ready to be correlated; 7) afterwards, from every $g_1^{\lambda g}, g_2^{\lambda g}, g_3^{\lambda g}, \dots, g_p^{\lambda g}$ WSSV filter image function is calculated and their corresponding K-Law nonlinear operation getting the $g_q^{\lambda g}(u', v')$ intensity function in complex plane; 8) applying $t_{j,l}^{\lambda g}(u, v) \bullet g_q^{\lambda g}(u', v')$ K-Law cross correlation operation over tile intensity function and the complex conjugate of WSSV filter function it is possible to obtain a positive WSSV inclusion body identification, depending of correlation peak energy level; 9) the $KSC^{\lambda g}$ correlation peak value is obtained by inverse K-Law Fourier transform of the K-Law cross correlation operation and $|KSC^{\lambda g}|^2$ is applied to increase K-Law cross correlation

peak energy level reducing noise ratio; 10) comparing $|KSC^{\lambda g}|^2$ with a ζ discriminating correlation value, where ζ is calculated by the analysis of WSSV filter bank when the bank is built, it can be possible to make a WSSV identification, thus when the cross correlation peak is greater than ζ , a positive WSSV identification is effectuated, if not positive identification is done, then next WSSV inclusion body is analyzed; 11) however, if positive WSSV identification is done, the K-Law cross correlation peak is located at the center coordinate of $S(x^c, y^c)_s$ WSSV inclusion body identified, it is extracted from tile image and it is being ready to be analyzed by the KSCA second process and deep manner; 12) finally, a texture analysis of WSSV inclusion body identified is taking over by the i^{ss} spectral index classifier; if the index value is located inside a WSSV fringe a corroborating positive WSSV identification is done.

3. Results and discussion

To test algorithm, a set of 15 connective and epithelium tissue fields were digitalized from 5 shrimps (3 images per shrimp), like as shown in Fig. 1; each field was digitalized with a resolution of 2088×1550 pixels and was divides in 30 sub images (tiled), having a total of 450 sub-images from the 5 shrimps; taken without any additional preprocessing like illumination or contrast correction just the fusion technique developed by (Bueno-Ibarra et al., 2010); these set of sub-images were analyzed using the filter bank which was constructed previously

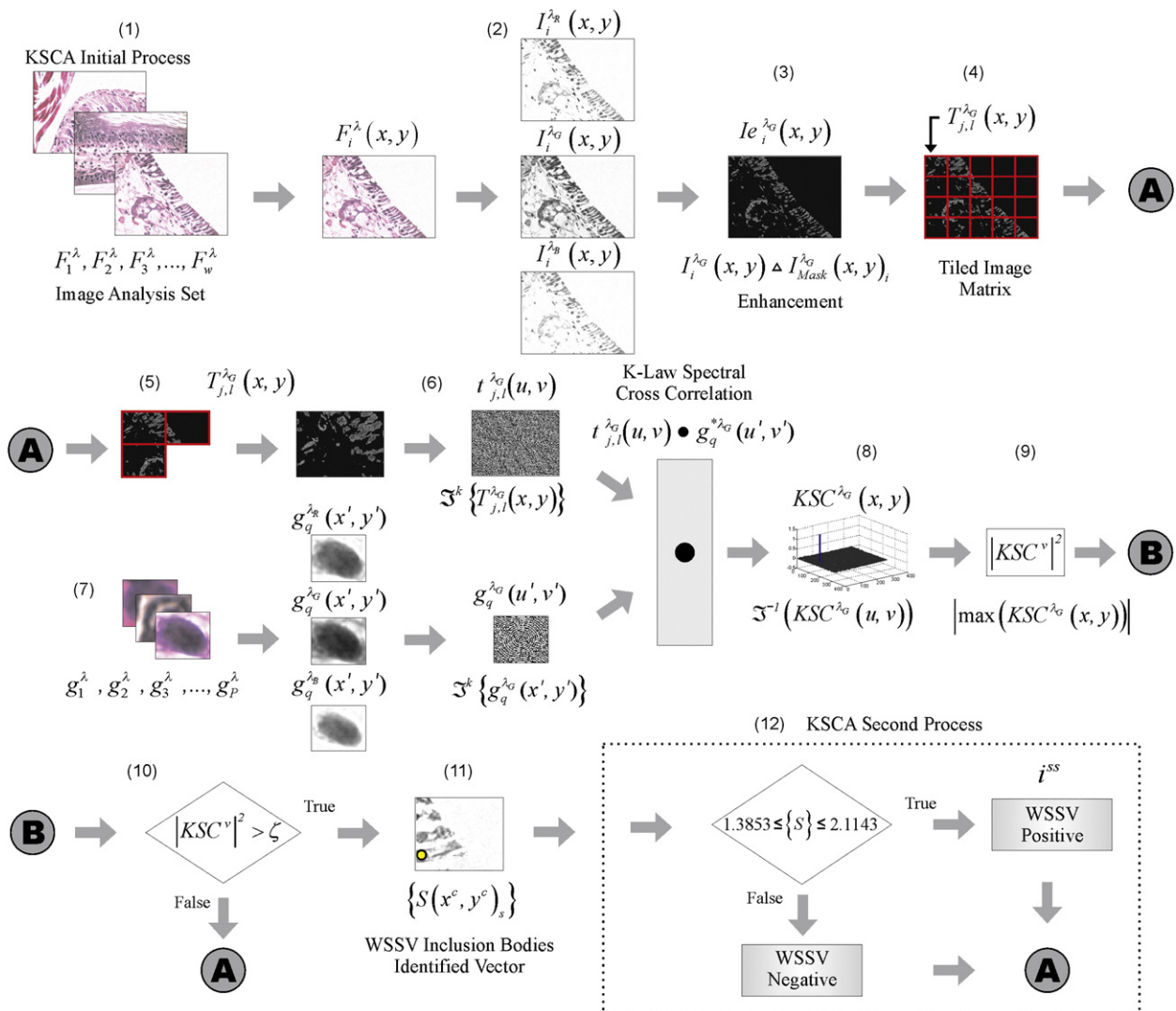


Fig. 5. KSCA process block diagram.

with 30 of the most characteristic and representative inclusion bodies which were selected from other group of slides.

A set of 15 microscope field samples digitalized images were acquired from 5 well know shrimp's connective epithelium tissues, like as shown in Fig. 1; at 2088×1550 pixels resolution; three digitalized images per organism were taken, without any additional preprocessing like illumination or contrast correction just the fusion technique developed by (Bueno-Ibarra et al., 2010); then from this set, 450 WSSV inclusion body tile images were processed; 30 most representative connective epithelium WSSV inclusion bodies were used to build a filter bank from where the identification is done.

After several numerical analyses from inclusion body samples a $\zeta = 0.257$ K-Law cross correlation threshold value and $\tau = 100$ enhancement threshold value were used to make the algorithm calculations. Fig. 6 shows examples of KSCA initial process analysis, where in row (a) were recognized real positive WSSV inclusion bodies; however in row (b) are shown some "possible" WSSV inclusion bodies. The last indicate that the KSCA system informs that several prospects have to be treated like positive WSSV hits, this result is due to the KSCA sensibility. That means that the system in this initial process has a level of error or doubts and it could be necessary to carry out deeper analysis, perhaps doing an in situ hybridization analysis to confirm the diagnosis, however following with the second step of the KSCA process, these particles will be discarded and the identification is more precise.

Table 1 shows the mean analysis values of WSSV identification, where in the first column shows the average of WSSV inclusion bodies manually counted, with a filter bank of 30 possible inclusion bodies; second column shows the average of KSCA initial process of WSSV positive identification; third column shows the average of the second discriminating process of hit counts by KSCA; finally fourth column shows the final diagnosis made to every shrimp; finally fourth column shows the final diagnosis made to every shrimp; where results made by KSCA are informed like (I) organism infected or (N) organism non-infected.

In Table 1, mean values obtained in second column are not surprising; much more particles are recognized by KSCA initial process like targets (possible particles to be a WSSV inclusion

Table 1

KSCA virus identification mean counting values of infected samples (I–IV) versus non-infected samples (V), including the sample status shown in column D.

| Shrimp | KSCA mean analysis (30 inclusion bodies filter bank) | | | D |
|----------------|--|---|---|---|
| | Average of manually counting WSSV inclusion bodies | KSCA initial process WSSV recognition count | KSCA second process WSSV positive count | |
| I | 16.0 | 68.0 | 4.7 | I |
| II | 24.3 | 28.3 | 6.0 | I |
| III | 14.3 | 24.7 | 5.3 | I |
| IV | 23.0 | 68.0 | 5.0 | I |
| V ^a | – | 8.0 | 0.7 | N |

^a Shrimp with non-infected tissues.

body), however in deeper analysis KSCA second process these particles are discarded.

Analyzing the KSCA discrimination performance by a rapid mean analysis in WSSV positive recognition diagnosis (Infected shrimp samples I to IV and non-infected shrimp sample V, mean values shown in Table 1), there is a well defined calculated infected threshold value of $4.681 \leq \bar{x}_{Infected}$ with $(-2SE)$; thus WSSV infected region values are $\bar{x}_{Infected} = 5.25$, $\sigma_{Infected} = 0.569$ and $SE = 0.285$ where these values are mean, standard deviation and standard error respectively. Non-infected region mean value is $\bar{x}_{Non-Infected} = 0.7$ clearly it can be inferred that the KSCA has suitable discriminating performance; infected versus non-infected tissue analysis.

However to confirm these thoughts, a multiple comparisons single factor analysis of variance ANOVA with a significance level value of $\alpha = 0.05$ to reject or accept the null hypothesis and Honest Significant Difference HSD Tukey rank test (Pérez et al., 2005) are made over positive virus identification values shown in Table 1; $H_0: \mu_I = \mu_{II} = \mu_{III} = \mu_{IV} = \mu_V$ and $H_A: \mu_I \neq \mu_{II} \neq \mu_{III} \neq \mu_{IV} \neq \mu_V$, thus null hypothesis means that no differences exist in KSCA second analysis, whereas alternative hypothesis means that significant difference exists between each organism analysis made by KSCA.

The critical value of this test is $F_{\alpha(1), (k-1), (N-k)}$, where α is significance level value with $(P < 0.0005)$, $k = 5$ organism groups tested and $N = 15$ (WSSV inclusion bodies) counting data by images

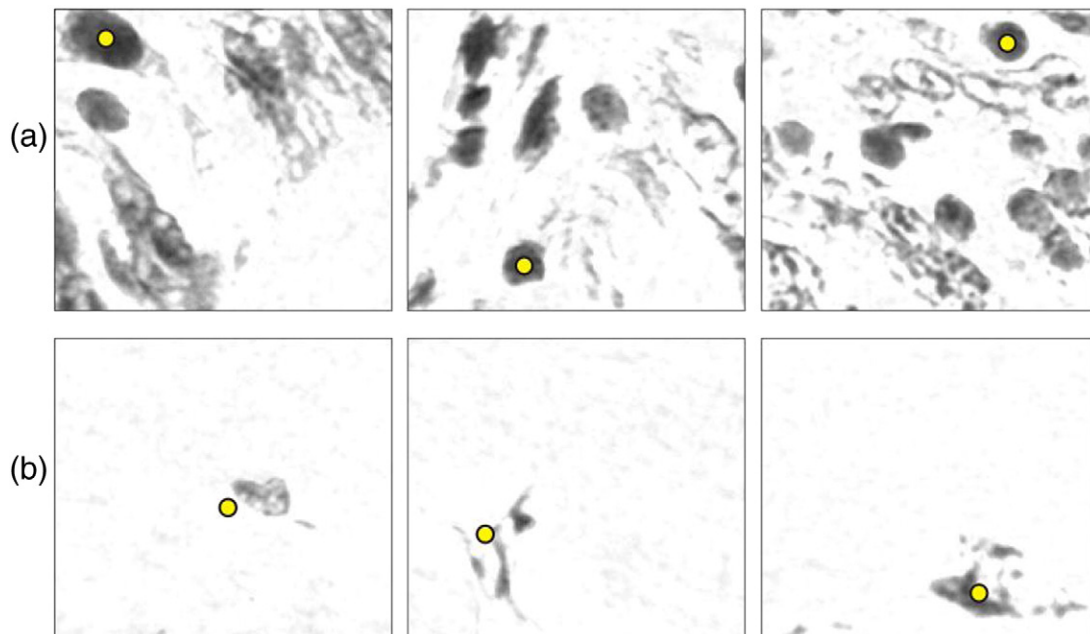


Fig. 6. (a) Real WSSV positive inclusion bodies recognized; (b) Possible WSSV inclusion bodies recognized; however deep analysis is needed to be done to these particles by the KSCA second process to confirm the diagnosis.

Table 2

HSD Tukey multiple comparisons test ranked by means; third column shows the calculated q values versus the critical $q_{(\alpha),(\nu),(k)}$ value for Tukey rank test and fourth column the acceptance or rejection of null hypothesis according to $q_{Calc} > q_{(\alpha),(\nu),(k)}$.

| Comparisons | Difference $\bar{x}_{\beta_2} - \bar{x}_{\beta_1}$ | q_{Calc} | $q_{(0.05),(10),(5)}$ | Conclusion |
|------------------------|--|------------|-----------------------|-----------------------|
| II vs. V ^a | 6.0 – 0.7 = 5.3 | 6.89 | 4.654 | Reject H ₀ |
| II vs. I | 6.0 – 4.7 = 1.3 | 1.72 | 4.654 | Accept H ₀ |
| II vs. IV | 6.0 – 5.0 = 1.0 | 1.29 | 4.654 | Accept H ₀ |
| II vs. III | 6.0 – 5.3 = 0.7 | 0.86 | 4.654 | Accept H ₀ |
| III vs. V ^a | 5.3 – 0.7 = 4.7 | 6.02 | 4.654 | Reject H ₀ |
| III vs. I | 5.3 – 4.7 = 0.7 | 0.86 | 4.654 | Accept H ₀ |
| III vs. IV | 5.3 – 5.0 = 0.3 | 0.43 | 4.654 | Accept H ₀ |
| IV vs. V ^a | 5.0 – 0.7 = 4.3 | 5.59 | 4.654 | Reject H ₀ |
| IV vs. I | 5.0 – 4.7 = 0.3 | 0.43 | 4.654 | Accept H ₀ |
| I vs. V ^a | 4.7 – 0.7 = 4.0 | 5.16 | 4.654 | Reject H ₀ |

^a Shrimp with non-infected tissues.

analyzed. Null hypothesis is rejected if the calculated F is greater than critical value $F_{\alpha(0.05),(4),(10)} = 3.48$; thus in this test null hypothesis is rejected, but just can be concluded that difference exists between mean values, therefore for this analysis this is correct, however it is needed to be proven that mean value of non infected tissue has a significant difference compared to other infected mean values.

Hence, a HSD Tukey rank test is applied to compare each mean value; WSSV positive diagnoses are ranked by means.

Multiple comparisons are made by $k(k-1)/2 = 10$ possible combinations to test each pairwise $H_0: \mu_{\beta_2} = \mu_{\beta_1}$, null hypothesis versus $H_A: \mu_{\beta_2} \neq \mu_{\beta_1}$, alternative hypothesis; β_1, β_2 index are pairwise organisms mean values compared.

Table 2 shows the HSD Tukey rank test summary analysis to prove the existence of significant mean value difference of non infected tissue to other mean values. First column shows the comparison of possible combinations; second column shows the pairwise mean values comparison by descendant order; third column shows the calculated q values by $(\bar{x}_{\beta_2} - \bar{x}_{\beta_1}) / SE$; where $SE = \sqrt{MSE / N_{Images \text{ per Shrimp}}} = 0.7746$ for this analysis, where MSE is the mean square error; fourth column shows a critical $q_{(\alpha),(\nu),(k)}$ value for Tukey rank test, where it is dependent upon $\alpha = 0.05$, ν is defined as error, degrees of freedom DF from the analysis of variance and k total number of means being tested, thus $q_{(0.05),(10),(5)} = 4.654$; finally, fifth column shows the results of Tukey rank test about null hypotheses rejection.

4. Conclusions

This paper presents a new algorithm to identify representative groups of digitalized images of WSSV inclusion bodies from histology slides, taken from several organs of infected shrimps. The Fourier K-Law non-linear filter technique exploits important WSSV characteristics by the analysis of frequencies.

Hence, by the results obtained in Table 2 the overall conclusion is the average between infected samples (I to IV) versus non-infected samples (V) with mean values $\mu_I = \mu_{II} = \mu_{III} = \mu_{IV} \neq \mu_V$, clearly supports the existence of a significant difference by KSCA analysis,

thus KSCA can be useful like a preliminary tool to analyze hundreds of shrimp samples in automatic way.

Future work can be done in the application of the KSCA in new tissue samples obtained by other organisms where the virus has a different pattern and its identification is more complex; however it is necessary to characterize and built a new filter bank.

Finally, the potential of this algorithm can be used to analyze and identify other kind of shrimp's viruses and/or other animal or human virus complex patterns.

Acknowledgments

This document is based on work partially supported by CONACYT under Grant no. 102007.

References

- Álvarez-Borrego, J., Chávez-Sánchez, M.C., 2001. Detection of IHNN virus in shrimp tissue by digital color correlation. *Aquaculture* 194, 1–9.
- Bell, T.A., Lightner, D.V., 1988. *A Handbook of Normal Shrimp Histology Special Publication No. 1*. World Aquaculture Society, Baton Rouge, LA, USA.
- Bueno-Ibarra, M.A., Álvarez-Borrego, J., Acho, L., Chávez-Sánchez, M.C., 2005a. Fast autofocus algorithm for automatized microscopes. *Opt. Eng.* 44 (6) 063601-1.
- Bueno-Ibarra, M.A., Álvarez-Borrego, J., Acho, L., Chávez-Sánchez, M.C., 2005b. Polychromatic image fusion algorithm and fusion metric for automatized microscopes. *Opt. Eng.* 44 (9) 093201-1.
- Bueno-Ibarra, M.A., Chávez-Sánchez, M.C., Álvarez-Borrego, J., 2010. Development of nonlinear K-law spectral signature index to classify white spot syndrome virus basophilic inclusion bodies. *BioSciencesWorld, Proceedings of IEEE Computer Society, The First International Conference on Advances in Bioinformatics and Application*, pp. 30–33.
- Coronel-Beltrán, J., Álvarez-Borrego, J., 2010. Comparative analysis between different font types and styles letters using a nonlinear invariant digital correlation. *J. Mod. Opt.* 57 (1), 58–64.
- González-Fraga, J.A., Kober, V., Álvarez-Borrego, J., 2006. Adaptive SDF filters for pattern recognition. *Opt. Eng.* 45, 057005.
- Lightner, D.V., 1996. *A handbook on shrimp pathology and diagnostic procedures for diseases of cultured penaeid shrimp*. World Aquaculture Society, Baton Rouge, LA, USA.
- Lightner, D.V., Pantoja, C.R., 2001. *A handbook of penaeid shrimp diseases and diagnostic methods* (English and Spanish versions). A publication in cooperation between the University of Arizona and United States Department of Agriculture (USDA-USAID-CSREES), as part of the Hurricane Mitch Reconstruction Program of Central America, pp. 48–57 (Spanish version).
- Lightner, D.V., Redman, R.M., 1998. *Shrimp diseases and current diagnostic methods*. *Aquaculture* 164, 201–220.
- Millán, M.S., Yzuel, M.J., Campos, J., Ferreira, C., 1992. Different strategies in optical recognition of polychromatic images. *Appl. Opt.* 31 (14), 2560–2567.
- Mouriño-Pérez, R.R., Álvarez-Borrego, J., Gallardo-Escárate, C., 2006. Digital color correlation for the recognition of *Vibrio cholerae* O1 in laboratory and environmental samples. *Mar. Biol. Oceanogr.* 41 (1), 77–86.
- OIE, 2010. Manual of diagnostic test for aquatic animals. http://www.oie.int/eng/normes/fmanual/A_summry.htm.
- Pérez, F., Volckaert, F.A.M., Calderón, J., 2005. Pathogenicity of white spot syndrome virus on postlarvae and juveniles of *Penaeus* (*Litopenaeus*) *vannamei*. *Aquaculture* 250, 586–591.
- Poulos, B.T., Pantoja, C.R., Bradley-Dunlop, D., Aguilar, J., Lightner, D.V., 2001. Development and application of monoclonal antibodies for the detection of white spot syndrome virus of penaeid shrimp. *Dis. Aquat. Org.* 47, 13–23.
- Solorza, S., Álvarez-Borrego, J., 2010. Digital system of invariant correlation to position and rotation. *Opt. Commun.* 283 (19), 3613–3630.
- Walker, P.J., Mohan, C.V., 2009. Viral disease emergence in shrimp aquaculture: origins, impact and the effectiveness of health management strategies. *Rev. Aquac.* 1, 125–154.